# Durability of the hydrophobic treatment on brick and mortar

Soulios, Vasilis; de Place Hansen, Ernst Jan; Peuhkuri, Ruut Hannele; Møller, Eva B.; Ghanbari-Siahkali, Afshan

*Published in:*
Building and Environment

*DOI (link to publication from Publisher):*
10.1016/j.buildenv.2021.107994



*Publication date:*
2021

*Document Version*
Publisher's PDF, also known as Version of record

Building and Environment 201 (2021) 107994

Contents lists available at ScienceDirect

Building and Environment

journal homepage: www.elsevier.com/locate/buildenv

# Durability of the hydrophobic treatment on brick and mortar

Vasilis Soulios [a,*], Ernst Jan de Place Hansen [a], Ruut Peuhkuri [a], Eva Møller [b], Afshin Ghanbari-Siahkali [c]

[a] Department of the Built Environment, Aalborg University, Denmark
[b] DTU Civil Engineering, Technical University of Denmark, Kgs. Lyngby, Denmark
[c] Danish Technological Institute, Gregersensvej, Taastrup, Denmark

A B S T R A C T

Hydrophobization lessens the water absorption by facade materials and is thus presumed to reduce moisture problems in internally insulated facades. However, to do this it should retain the water repellency performance throughout aging. The aim of this study is to evaluate the impact of aging on the durability of the hydrophobic treatment on bricks and mortars. The resulting absorption coefficient, after 635 repeating artificial aging cycles of alternating UV radiation (102 min) and water exposure (18 min) reveals that the hydrophobic layer maintains its water repellency performance both in brick and mortar. The samples were treated with two different water repellent agents in different concentrations and tested for capillary water uptake. Additionally, the findings show that cycles of weathering could contribute positively to further reduction of the absorption coefficient of hydrophobized brick and mortar samples. Subsequently, Karsten tube tests on samples from artificial aging illustrate the same water repellency performance as mock-up walls exposed to ambient conditions, six years after being hydrophobized. Contact angle measurements before and after artificial aging reveal that the beading effect declines through aging. However, the beading effect seems to be just a surface effect affected by UV-light. Moreover, after aging, hydrophobized brick and mortar samples, tested by visual inspection, maintain their appearance while untreated samples show signs of efflorescence. In total, these findings indicate that the water uptake of hydrophobized brick or mortar remains very low after aging including water spraying and UV light.

## 1. Introduction

Denmark is targeting to be independent of fossil fuels by the year 2050 [1]. In the EU, existing buildings represent 99% of the building stock [2], which accounts for about 40% of the total energy consumption [3]. 10%–40% of these buildings [4] are historical, high energy-consuming buildings [3,5–7]. The household's energy consumption within EU-27 is dominated by space heating in a percentage of 67% [8]. Often such buildings have worth preserving solid facades, making internal insulation the only feasible technique for thermal insulation [9]. Internal insulation itself can reduce the heat losses of a wall by 76% in the case of mineral wool plus vapor barrier and 63% in the case of CaSi, in a climate like Copenhagen [10]. However, internal insulation may lead to moisture-related problems [4,5,11–14]. The main source of the problems derives from the accumulated moisture load from wind-driven rain [15,16], and internal insulation negatively affects the drying potential of the masonry wall [12,17–19]. Studies comparing the overall hygrothermal performance of internally insulated solid masonry walls, tend to suggest vapor open and capillary active internal insulation systems to counterbalance the reduced inward drying [5,20]. However, applying water repellent agent in the internally insulated wall practically eliminates the absorption of the wind-driven rain [21–24].

Moisture transfer in building materials plays a vital role in the durability and thereby sustainability of built structures [12,25,26]. Absorption of moisture is the main mechanism for the deterioration of porous building materials and the starting point for many moisture-related damages in the building structure potentially affecting the durability. Moreover, absorption of moisture increases the thermal conductivity of building components resulting in increased heat losses [10,21]. So, water absorption that remains at low levels over time enhances the durability of the porous building materials and consequently the durability of the whole structure. Hydrophobization is proven to significantly reduce the absorption coefficient of both brick and mortar and at the same time to allow water vapor diffusion, thus not fully impeding the drying of the material [21,22]. But there is very little experience in the literature about the durability of the hydrophobic treatment of brick masonry and brick and mortar samples, especially regarding the possible changes of the absorption coefficient of hydrophobized brick and mortar. Some studies however, have used Karsten tube tests to measure water uptake on hydrophobized aged masonry [27,28] and on aged brick and natural stone samples [29]. White efflorescence is widely known as an aesthetic problem of brick masonry, where

* Corresponding author.
E-mail addresses: vsou@build.aau.dk, v.soulios@ihu.edu.gr (V. Soulios).

https://doi.org/10.1016/j.buildenv.2021.107994
Received 19 March 2021; Received in revised form 20 May 2021; Accepted 21 May 2021
Available online 26 May 2021

water transport plays an essential role [30,31]. Concrete impregnated with a water repellent agent in cream form illustrates resistance against salt formation [32] but there are no similar studies for brick and mortar. Each of these factors highlights the need to investigate the durability of hydrophobized masonry and prior to that, the durability of masonry components, i.e. hydrophobized brick and mortar samples, expressed by the absorption coefficient, as well as the appearance of the hydrophobized materials after aging. Moreover, even though contact angle measurement is not a precise indicator to assess the water repellency performance [33], comparing the contact angle in hydrophobized materials before and after artificial aging could provide information on the influence of the aging on the beading effect.

By providing an artificial aging test with hydrophobized brick and mortar samples this paper aims to meet this need. It begins by describing the building materials and water repellent agents used for this study as well as describing the methodology for artificial aging and the experiments conducted to investigate water absorption, beading effect, and discoloration through aging. This is followed by a section presenting how the absorption coefficient of the hydrophobized materials develops after several rounds of repeating cycles of artificial aging. A supplementary section, using Karsten tube tests, compares the water uptake of the samples used in the artificial aging with mock-up walls constructed with the same building materials. A subsequent section presents results from contact angle measurements on hydrophobized samples before and after artificial aging. It also considers the discoloration of untreated samples after artificial aging. Finally, the paper discusses the results, contrasting them with previous work.

## 2. Materials and methods

### *2.1. Target building materials*

The building materials used in the current study were selected to represent building materials to be found in a typical Danish building from before 1950 (see Table 1); soft-molded brick and air-lime mortar. Further, cement mortar was included, as it is common practice in Denmark to perform repointing of mortar joints before impregnation, normally with cement mortar.

The yellow soft-molded brick from Helligsø Teglvaerk in Denmark imitates a historic Danish brick and its properties have been thoroughly analyzed [10,21,22,34–37]. Further, historic brick samples were obtained from an old building in Denmark constructed in 1944 in order to test a brick that was exposed to actual weathering before hydrophobization. Material properties of the historic brick could be found in Refs. [10,21].

Most of the old masonry buildings in Denmark have been constructed with air lime mortar. The air lime mortar used in this study was supplied as ready-mix from Wewers and mixed with tap water to form fresh mortar which was placed in molds for casting. In order to imitate the mortar being placed towards bricks as in a brick masonry, wound cleaning swabs were placed at both sides of the molds (top and bottom) and the samples were placed in a climatic chamber (65% RH, 20 °C) for one month [38]. For the air lime mortar samples to represent a historic type of air lime mortar that has been part of brick masonry for many years [39], the samples were placed in a carbonation chamber (1% $CO_2$ exposure) for three months. The air lime mortar samples were tested with phenolphthalein and they were fully carbonated.

The type of cement mortar supplied from Wewers is the one that is usually used to repoint mortar joints in Denmark and has not been carbonated in order to represent a fresh cement mortar used to re-point the mortar joints before impregnation.

The size of the tested samples was 2 × 5 × 15 cm to fit the Atlas weather-ometer (see section 2.4 Experimental set-up).

### *2.2. Selected water repellent agents*

The selected water repellent agents (Table 2) are ready-to-use, in cream form, as cream products are widely used nowadays due to their easy application and long contact time that requires just a single treatment [21]. Further, liquid and cream-based products are shown to have the same effect in terms of water repellency on brick and mortar samples [21]. Funcosil Remmers FC cream is a water-based silane cream, recommended for mineral substrates, that can be ordered in any possible concentration [40], but commonly used in Denmark with a 40% concentration. The Wacker BS cream C is a water-based silane cream in 80% concentration that is recommended for concrete [41].

**Table 1**
Building materials used in the current study.

| Name | Description |
|---|---|
| Y brick | Yellow soft-molded Danish brick from Helligsø Teglværk |
| H brick | Historic Danish Brick from an old building in Copenhagen (1944) |
| AL mortar | Carbonated air lime mortar with aggregates of 0–4 mm grain size (7.7%) (Wewers) |
| C mortar | Cement mortar with aggregates of 0–4 mm grain size (Wewers) |

**Table 2**
Water repellent agents used in the current study.

| Product | Company | Type | Form | Diluent | Concentration | Substrate |
|---|---|---|---|---|---|---|
| FC | Remmers | Silane | Cream | Water | 40% | Mineral |
| BS | Wacker | Silane | Cream | Water | 80% | Concrete |

Information derived from the technical data sheets of the products. Both water repellent agents are mainly silane but they contain small percentage of siloxane.

**Table 3**
Laboratory experiments. Test plan including measured properties, type of tests, sample size and amount, type of material, and water repellent agent.

| Material (No. of samples for each type) | Treatment | 0 cycles | 165 cycles | 335 cycles | 482 cycles | 635 cycles |
|---|---|---|---|---|---|---|
| **Water absorption coefficient ($A_{cap}$) by capillary water uptake (2 × 5x15 cm samples)** | | | | | | |
| Y brick, H brick, AL mortar, C mortar (3) | Untreated | X | | | | X |
| Y brick, H brick, AL mortar, C mortar (3) | FC 40% | X | X | X | X | X |
| Y brick, H brick, AL mortar, C mortar (3) | BS 80% | X | X | X | X | X |
| **Water absorption by Karsten tube (2 × 5 × 15 cm samples)** | | | | | | |
| Y brick, H brick, AL mortar, C mortar (3) | Untreated | | | | | X |
| Y brick, H brick, AL mortar, C mortar (3) | FC 40% | | | | | X |
| Y brick, H brick, AL mortar, C mortar (3) | BS 80% | | | | | X |
| **Water absorption by Karsten tube (1 × 2 m walls)** | | | | | | |
| Y brick and AL mortar mock-up walls (3) | Untreated<br>FC 40% | Tested at mock-up walls, exposed outdoor for 6 years before Karsten tube test | | | | |
| **Contact angle (γ) by dropsnake method (2 × 5 × 15 cm samples)** | | | | | | |
| Y brick, H brick, AL mortar, C mortar (3) | Untreated | | | | | |
| Y brick, H brick, AL mortar, C mortar (3) | FC 40% | X | | | | X |
| Y brick, H brick, AL mortar, C mortar (3) | BS 80% | X | | | | X |
| **Discoloration by visual inspection (2 × 5 × 15 cm samples)** | | | | | | |
| Y brick, H brick, AL mortar, C mortar (3) | Untreated | X | | | | X |
| Y brick, H brick, AL mortar, C mortar (3) | FC 40% | X | | | | X |
| Y brick, H brick, AL mortar, C mortar (3) | BS 80% | X | | | | X |

### 2.3. Hydrophobic treatment

Samples of all types were cleaned with a brush to remove dirt and dust and washed with deionized water to prevent absorption of extra salts. Then, they were stored in an oven at 55 °C, so that moisture from the intense water exposure could evaporate. When reached a stable weight (after 4–5 days), the samples were cooled down to room temperature. For impregnation with cream products the minimum recommended amount, 150–200 ml/m$^2$, was applied with a brush [40]. Only one face (5 × 15 cm) was treated with a water repellent agent. The opposite face was left untreated, while the four smaller faces were waterproofed with epoxy resin. Finally, the samples were stored at room temperature and relative humidity for one month of curing.

### 2.4. Experimental set-up

The durability of the hydrophobic layer was characterized by the ability to repel liquid water and the ability to keep the substrate clean from dirt and possible efflorescence. Table 3 describes how the study has been conducted.

To evaluate the durability of the hydrophobic surface treatment on brick and mortar, artificial aging was conducted, according to ISO 4892–2 [42], with Atlas Ci 4000 weather-ometer, at the Danish Technological Institute, Taastrup (Fig. 1). ISO 4892 [42] is targeted at the durability of plastics but its key features (UV radiation and water spray) are in line with [29], also performing artificial weathering of hydrophobized porous building materials in Atlas weather ometer. The samples were placed in plastic holders that cover the edges (from the 75 cm$^2$ of the samples' face surface, only 57.8 cm$^2$ are exposed to water spray and UV radiation). The plastic holders were placed on a carousel, inside a climatic chamber. The samples were exposed to sprayed water and UV radiation only from the interior of the carousel. The water repellency performance is evaluated by the water absorption coefficient ($A_{cap}$) of the samples, obtained via water uptake tests in accordance with [43], as described in Refs. [44,45]. The samples were placed in a plastic container with deionized water that covered less than one cm of the sample, over plastic net support, for 1-D free capillary water uptake. The mass of the sample was determined with a balance reading 0.001 g and the samples were wiped with wet paper before each measurement. Since impregnation decreases the rate of capillary water uptake, the water uptake tests for the impregnated samples lasted for 24 h and the time intervals for the measurements were: 10′, 30′, 1h, 1h 30′, 2h, 3h, 4h, 7h, 9h, and 24h. When displaying water uptake in kg/m$^2$ towards $\sqrt{\text{seconds}}$ does not produce a straight line but a curve of some form, $A_{cap}$ is defined as the increase in weight (Δm) in kg/m$^2$ at 24h divided by $\sqrt{86400}$ [43].

$$A_{cap} = \frac{\Delta m}{\sqrt{86400}} \tag{1}$$

For the untreated samples, the water absorption coefficient was measured before and after artificial aging. For the treated samples, capillary water uptake tests were carried out one month after the application of the water repellent agent, during artificial aging (every two weeks), and after artificial aging. Before each measurement, the samples were dried in an oven at 55 °C and then cooled down at room temperature. Each result is an average based on three samples. The whole procedure of artificial aging consisted of 635 cycles and the water absorption coefficient measurements were carried out after 165, 335, 482, and 635 cycles. One cycle consisted of:

102 min: Lamp Xennon
- Irradiance level: 0.5 W/m$^2$ at 340 nm (UV)
- Back panel temperature: 63 °C
- Chamber temperature: 38 °C
- Relative humidity: 50%
- Specimen water spray: off
- Back water spray: off

18 min: Specimen water spray (deionized): 0.2 L/min, pressure: 138–344 kPa (20–30 psi)
- The rest of the weathering test conditions remained the same

The 635 cycles used in the present study were selected to represent similar exposure hours to UV radiation and water spray as in De Witte [29]. There is no official equivalence of the artificial cycles to actual years.

As a first approach to translate the artificial weathering cycles to actual years, vertical Karsten tube tests were conducted on the samples after 635 cycles. The results were compared with horizontal Karsten tube tests, conducted on bricks and mortar joints (covering also a small area of brick) of mock-up walls constructed with Yellow brick and air lime mortar at the Technical University of Denmark and impregnated with FC 40% in February 2015 [37], about 6 years before the artificial aging test.

Both vertical and horizontal Karsten tube tests consist of a 30 mm diameter dome (3 cm$^2$ test area) attached to a glass tube of 10 cm head of water (15 ml volume), a pressure roughly corresponding to double the wind pressure of a hurricane. The Karsten tube is pasted onto the substrate to be tested using plasticine as a sealing material. The drop in the

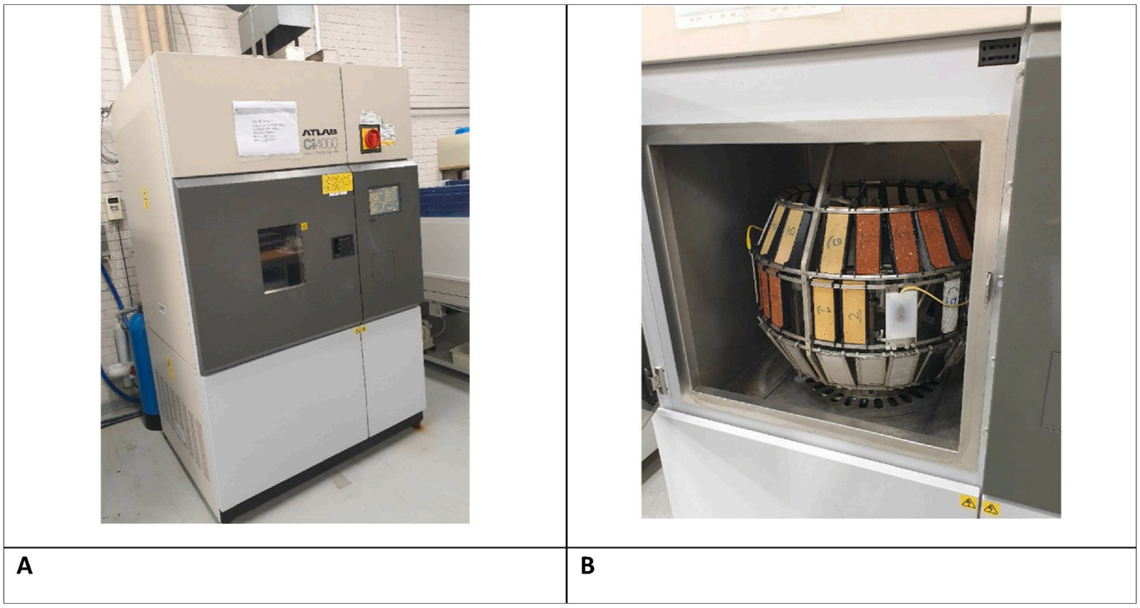


**Fig. 1.** Test setup for artificial aging. A) Atlas Ci4000 weather-ometer and B) test specimens on carousel sample holder inside the chamber.

water level is recorded every minute for 11 min and the water absorption in ml/min is calculated by taking the average of the last 10 measurements. The first minute is not taken into account, to avoid surface wetting to be included in the results. In order to maintain steady water pressure, the water in the tube is kept during the test by adding more water every time 1 ml of water is absorbed [46].

Contact angle measurements took place, as an indicator for the beading effect before and after artificial aging. The measurements were performed on 3 μl (microliter) water droplets placed on the treated surface of the materials via pipette. The shape of the droplets was recorded by a CCD camera and the resulting images were analyzed by DropSnake [47,48], a plugin for ImageJ software, similarly to Ref. [49]. The contact angles were measured immediately after the droplet fell on the surface.

The substrates of both untreated and treated samples were inspected visually for potential discoloration after the artificial aging.

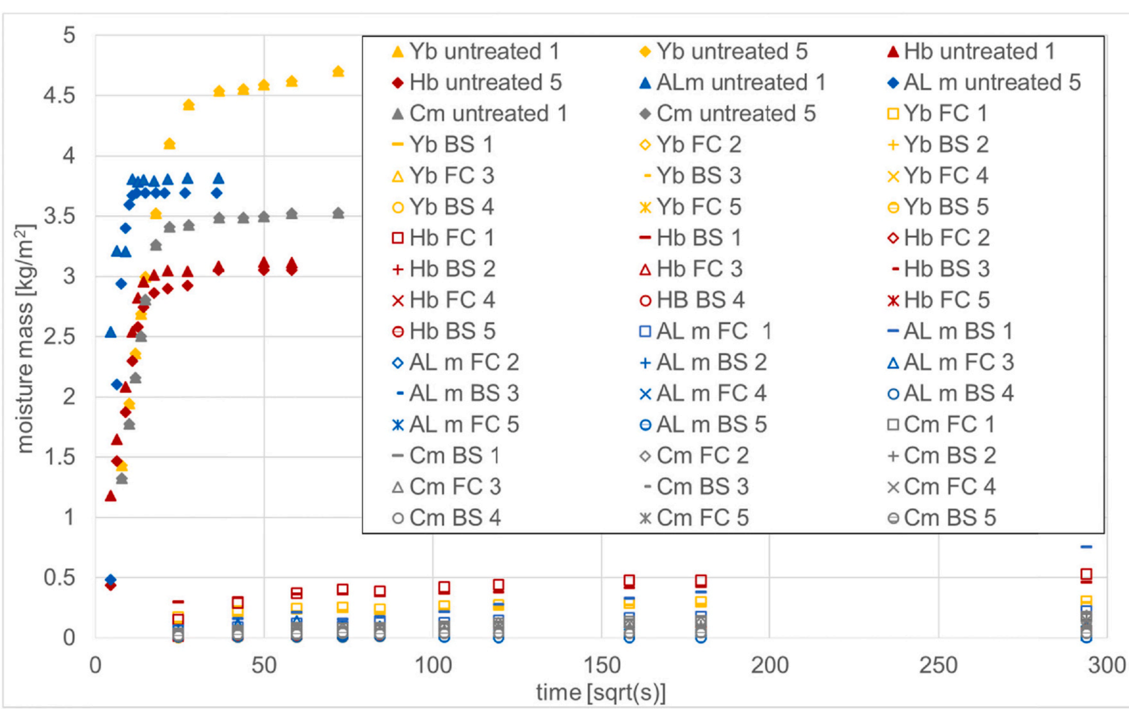


**Fig. 2.** Capillary water uptake of Y brick, H brick, C mortar, AL mortar, untreated and impregnated with Remmers FC cream 40% and Wacker BS cream C 80%. 1: 1st water uptake before artificial aging, 2: 2nd water uptake after 165 cycles of artificial aging, 3: 3rd water uptake test after 335 cycles of artificial aging, 4: 4th water uptake after 482 cycles of artificial aging, 5: 5th water uptake after 635 cycles of artificial aging. Each point of each curve is the average value of the respective measurements of three different samples.

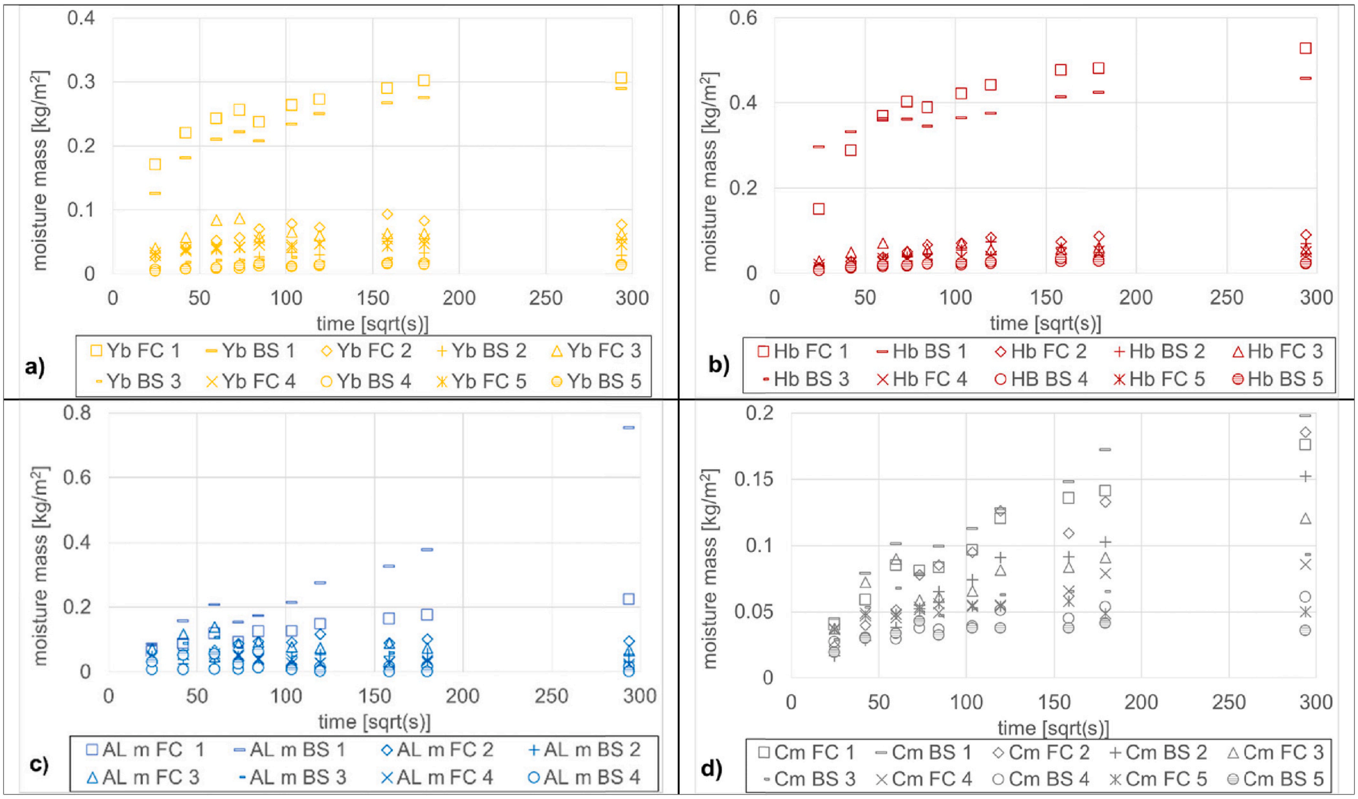


**Fig. 3.** Capillary water uptake of a) Y brick, b) H brick, c) AL mortar, d) C mortar, impregnated with Remmers FC cream 40% and Wacker BS cream C 80%.1: 1st water uptake before artificial aging, 2: 2nd water uptake after 165 cycles of artificial aging, 3: 3rd water uptake test after 335 cycles of artificial aging, 4: 4th water uptake after 482 cycles of artificial aging, 5: 5th water uptake after 635 cycles of artificial aging. Each point of each curve is the average value of the respective measurements of three different samples.

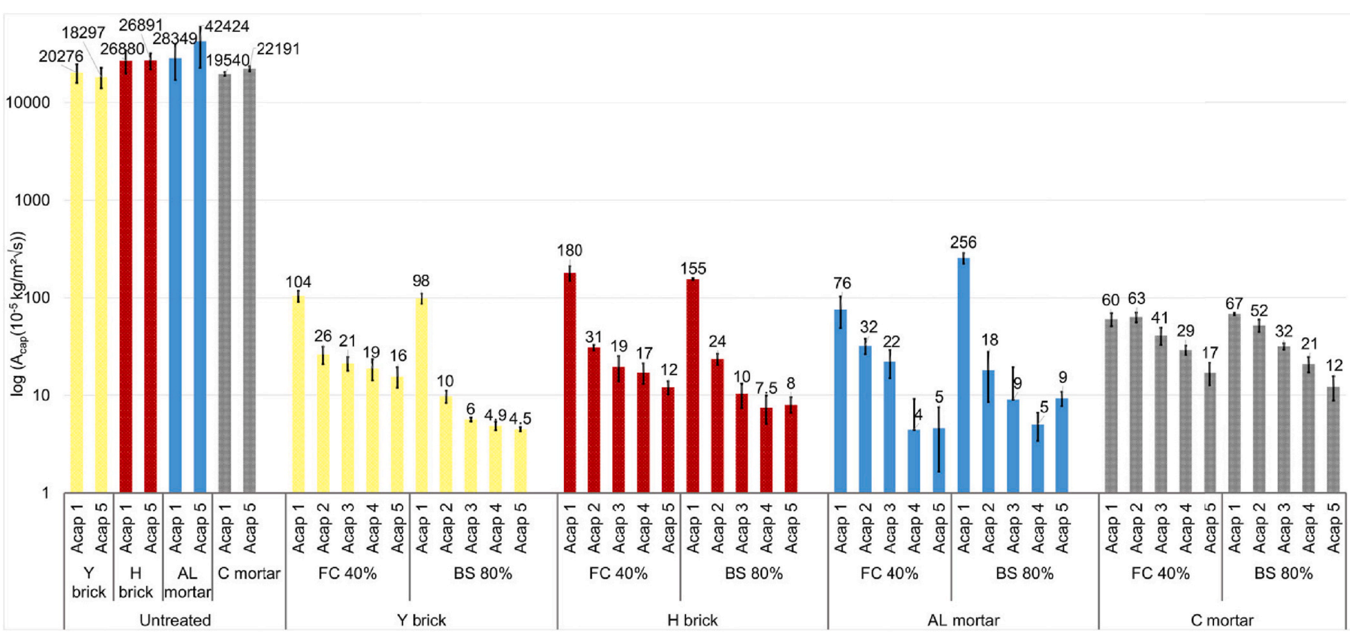


**Fig. 4.** Water absorption coefficient by capillary water uptake test of Y brick, H brick, AL mortar, C mortar, untreated and impregnated with Remmers FC cream 40% and Wacker BS cream C 80%. Acap 1: absorption coefficient before artificial aging, Acap 2: after 165 cycles of artificial aging, Acap 3: after 335 cycles of artificial aging, Acap 4: after 482 cycles of artificial aging, Acap 5: after 635 cycles of artificial aging. Each result is an average based on three samples, error bars correspond to standard deviation.

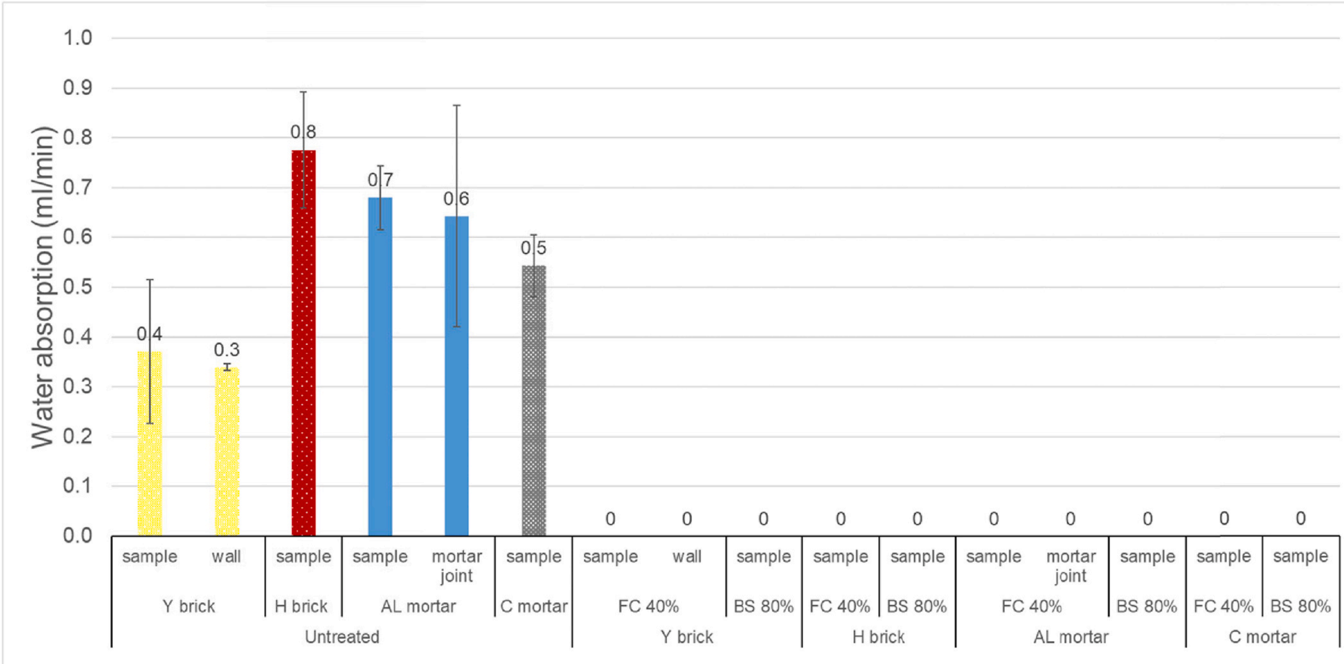


**Fig. 5.** Water absorption by Karsten tube test, Y brick, H brick, AL mortar, C mortar, and mock-up wall, untreated and impregnated with Remmers FC cream 40% and Wacker BS cream C 80%. "Sample" refers to samples from artificial aging, "wall" and "mortar joint" refer to mock-up wall measurements on brick and mortar joints respectively. Each result is an average based on three measurements, error bars correspond to standard deviation.

## 3. Results

### 3.1. Capillary water uptake test before/after artificial aging

Fig. 2 illustrate the capillary water uptake curves both of untreated and treated samples during the artificial weathering while Fig. 3 shows only the treated samples. The water uptake curves of all the treated samples were significantly reduced compared to untreated. The moisture mass difference against sqrt(s) did not give a straight line, but could follow a curve of some form (Fig. 3).

Fig. 4 focuses on the water absorption coefficient of the different samples during the testing period. The untreated samples did not show

**Table 4**
Water droplets in hydrophobized surfaces before and after artificial aging.

| | FC 40% | | BS 80% | |
|---|---|---|---|---|
| | Before aging | After aging | Before aging | After aging |
| Y Brick | 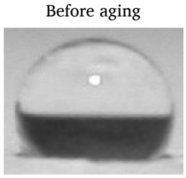 | 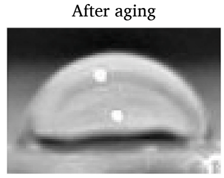 | 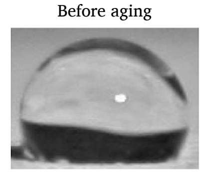 | 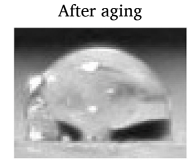 |
| H Brick | 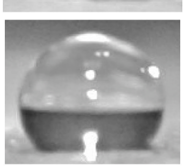 |  | 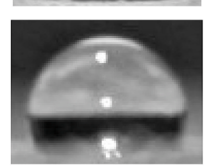 | 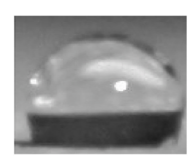 |
| C Mortar | 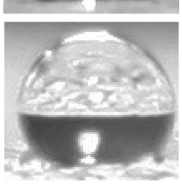 | | 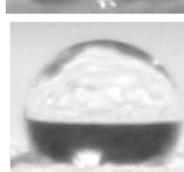 | 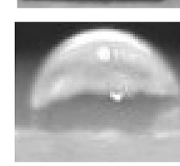 |
| AL mortar | 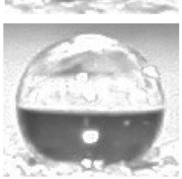 | | 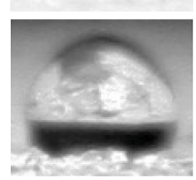 | 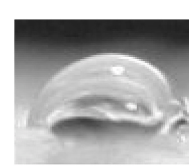 |

In the case of mortar samples treated with FC 40%, after aging, it was not possible to take a picture of the droplets, since they were not forming sufficient spherical droplets.

**Table 5**
Contact angle measurements before and after artificial aging.

| | Y brick | | H brick | | C mortar | | AL mortar | |
|---|---|---|---|---|---|---|---|---|
| | FC 40% | BS 80% | FC 40% | BS 80% | FC 40% | BS 80% | FC 40% | BS 80% |
| **Before aging (γ°)** | 130 (8) | 128 (4) | 124 (3) | 123 (1) | 130 (5) | 125 (7) | 132 (9) | 130 (9) |
| **After aging (γ°)** | 104 (4) | 111 (3) | 91 (15) | 121 (4) | | 111 (6) | | 109 (9) |

In the case of mortar samples treated with FC 40%, after aging, it was not possible to measure the contact angle of the droplets, since it was significantly reduced. Each result is an average based on three samples. The values in () correspond to the standard deviation.

significant changes in the water uptake after 635 cycles of aging. All treated samples showed reduced water uptake after treatment, and the water uptake was further reduced during the aging period.

The absorption coefficient on the first test before aging was reduced approximately by a factor of 200 due to hydrophobization (e.g Y brick treated with FC 40%, $A_{cap1}$: 0.00104 $kg/m^2s^{1/2}$ from untreated $A_{cap}$: 0.2 $kg/m^2s^{1/2}$) and was further reduced by a factor of more than 1000 ($A_{cap5}$: 0.00016 $kg/m^2s^{1/2}$) after aging for all the tested materials, compared to untreated. Consequently, the ability of the hydrophobization to reduce water uptake is not diminished by the performed artificial aging. The absorption coefficient seems to be positively influenced by artificial aging since it is further reduced during the process of repeated cycles.

### 3.2. Karsten tube measurements

The Karsten tube test, as an additional indicator, supported the observation that hydrophobization blocked liquid water transport even after aging in brick and mortar since the water penetrated neither samples nor brick and mortar joints of the mock-up wall hydrophobized six years ago (see Fig. 5). Also, the water absorption of untreated brick and mortar samples was similar to untreated bricks and mortar joints of the mock-up walls, as seen in Fig. 5.

### 3.3. Contact angle measurements

Contact angle measurements provide additional information for the surface behavior of the hydrophobized building materials. The level of contact angle was similar between brick and mortars but for all the materials there was a tendency of reduced contact angle after artificial aging. In the case of C mortar and AL mortar impregnated with FC 40% the contact angle after aging was significantly reduced, making the capture of the droplet image challenging (see Table 4 and Table 5).

### 3.4. Discoloration of untreated samples after aging

The exterior appearance of the treated substrates remains clear after artificial aging while the untreated samples reveal a discoloration (white stains) as shown in Table 6. The discoloration on the untreated mortar samples may not appear clearly on the pictures but it was noticeable by the naked eye.

## 4. Discussion

The present study examined the effect of accelerated weathering on untreated and hydrophobized brick and mortar samples. The results show that silicon-based water repellent agents in cream form can create a durable hydrophobic layer that maintains both its water repellency performance and its appearance through artificial aging (exposure to UV radiation and water spray) but loses its beading effect.

The absorption coefficient of the untreated samples was not significantly affected by artificial aging. For the hydrophobized samples, the absorption coefficient was negligible compared to that of the untreated, revealing more than 99% reduction for all the tested materials before, during, and after artificial aging. However, by carefully observing Fig. 4, the after-treatment water exposure and longer curing time appeared to improve the water repellency performance of hydrophobized samples, as absorption coefficient ($A_{cap}$) was further reduced, in all the tested materials, especially between first and second capillary water uptake, as also reported in Ref. [21].

Two different types of brick, one type of air lime mortar and one type of cement mortar, all representing materials present in historic Danish buildings, illustrated the same behavior in terms of water repellency during aging resulting in very low absorption coefficients. Although air lime does not contain hydroxylated surfaces, the active ingredient was able to form irreversible bonds with the pore walls of the air lime mortar, since mortar also contains sand that has hydroxylated surfaces and thus kept the very low absorption coefficient after accelerated weathering similar to hydraulic lime mortar [21] and cement mortar (Fig. 4).

The mock-up walls were built with the same types of brick and mortar that were used as the samples that underwent artificial aging. Moreover, they were impregnated six years earlier (Feb 2015) with a water repellent agent included in the artificial aging tests (FC 40%). Both the Y brick and AL mortar samples and the Y brick and AL mortar joints illustrated zero penetration of water when tested with Karsten tube (Fig. 5). This is an indication that the artificial aging cycles corresponded to at least 6 years in real life, with the limitation that the artificial cycles do not include frost cycles.

Karsten tube tests show that the hydrophobic layer of a lime plaster facade impregnated with liquid water repellent agents can stay durable and repel liquid water even after 50 years [27]. In line with these findings, van Hees [28] reported that the effectiveness of the hydrophobic treatment, with liquid products, can last even more than 30 years after testing with Karsten tube over 60 case studies in three different countries (Netherlands, Belgium, Italy), but the effectiveness of the treatment is quite variable even within one wall. Cream-based water repellent agents became commercially available in the early 2000s [21], after [40] was published but no studies on the durability of cream-based products on brick and mortar have been reported in the literature. Fig. 5 illustrates that treatment of masonry with cream-based water repellent agents also stayed durable and repelled liquid water in a mock-up wall impregnated six years ago. The results depicted in Figs. 4 and 5 are in agreement with a test of hydrophobized brick and natural stone samples in Atlas weather-ometer [29]; their performance did not decrease with aging, although it might decrease when concentrations of water repellent agents lower than recommended were used. According to tests including freeze-thaw cycles, which neither the current paper nor [29] include, impregnated concrete maintained its effectiveness in terms of water repellency, tested with capillary water uptake, after aging [50]. However, observations regarding concrete are not necessarily valid for mortar or especially brick, since they are quite different building materials.

Capillary water uptake and Karsten tube tests illustrated that hydrophobization blocked the liquid water absorption of brick and mortar and showed the effectiveness and durability of hydrophobization after artificial aging with water spray and UV-light. The water repellent agents used in this study contain emulsifiers that allow the active ingredient to be mixed with water as a ready-to-use mixture. After the application of the water repellent agent, hydrolysis and poly condensation take place, requiring the presence of water. With these processes, the alkoxy groups (-OH) of the active ingredient molecules create irreversible bonds with the pore walls of the building material and the alkyl

**Table 6**
Substrate appearance of Y brick, H brick, C mortar, AL mortar after 635 cycles of artificial aging.

| | Untreated | FC 40% | BS 80% |
|---|---|---|---|
| Y brick |  |  |  |
| H brick |  |  |  |
| C mortar |  |  |  |
| AL mortar |  | 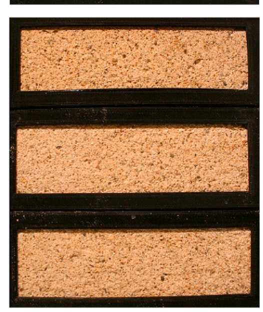 |  |

Each case is represented from 3 samples placed in the sample holder as it was located during the artificial weathering experiment except the AL mortar where the untreated and the treated with BS 80% is represented by two samples.

groups (-R) provide the hydrophobic properties to the compound. Wind driven rain will then "wash off" the emulsifiers and the active ingredient forms new bonds with the pore walls of the building material making the hydrophobic layer stronger, reducing the $A_{cap}$ further and inducing redistribution of the active ingredient deeper inside the material. Complementary to that, water coming from rain, or as a by-product of condensation reaction, acts as a reactant in the first part of polymerization (hydrolysis) [51]. Over time, this effect becomes less noticeable, since there is less active ingredient to form new bonds with the pore walls of the building material [21].

However, the four tested substrates showed a tendency of contact angle reduction after artificial aging that caused a declined beading effect (droplet formation on the facade during rain events). The contact angle reduction was more obvious to the cream with a lower concentration (40%) (Tables 4 and 5). The sample holders covered the edges of the samples (4.5 mm thickness). In this area, which was not exposed to UV radiation, the contact angle was not reduced after artificial aging in any sample. Since the whole surface of the samples was exposed five times to water uptake for 24 h, there was an indication that the exposure to UV radiation and not the exposure to water was responsible for the reduction of the beading effect after aging.

UV radiation, due to its high energy, can cause the formation of free radicals (i.e. molecules with an excess of electrons), which can cause degradation on polymeric surfaces [52]. The hydrophobic effect can be broken down by UV radiation, as manifested by the gradual decrease of the contact angle on the substrate (reduced beading effect). In concrete, UV light has been reported to break the Si–O–Si bonds between hydrophobic molecules and the substrate [50]. However, this only occurs in the outermost layer of the substrate, since UV light cannot penetrate deeper in the material [53]. UV radiation was not critical in terms of water absorption performance, because the Si–O–Si bonds remained intact in the subsurface [50] of brick and mortar, and liquid water did not penetrate into the materials (see Figs. 4 and 5). After aging, the exterior surface of the substrate may lose its hydrophobicity, although the inner layers of the building material keep their hydrophobic properties. Complementary to the current study, spectroscopic and microscopic techniques could be performed in order to investigate further the influence of UV radiation to the hydrophobic treatment.

The beading effect is not necessarily an indicator of good hydrophobic treatment and is not always desirable for the building owner, who wants to maintain the exact appearance and visual behavior of the facade (personal communication with Corne van Hamont, Wacker's representative). However, the beading effect could last longer by applying a higher percentage of siloxane [21] and higher concentrations of the active ingredient (see Table 5).

Artificial aging revealed that hydrophobization acts positively in retaining the exterior appearance of the samples since contrary to treated samples, all the untreated samples revealed white stains (efflorescence) after artificial aging (see Table 4). The migration of salts to the exterior surface is due to salts present inside the materials since the samples were sprayed with deionized water during the artificial aging. Efflorescence should be avoided as it is an aesthetic problem that harms the prestige of the building [30].

Mortar joints are regarded as the weak point of a masonry facade [28], however, they are not easy to characterize with a Karsten tube test. During Karsten tube tests on the mock-up wall (Fig. 5) it was challenging to adjust the glass tube on the mortar joints without having leakages. Especially, in buildings with concave mortar joints, it would be very difficult to test the water uptake with the Karsten tube test. Karsten tube is an accurate method for testing water uptake on bricks but it is more difficult to give accurate results on mortar joints [54]. Additional in-situ measurement equipment, not available for this study, covers wider wall areas [55]. However, the impregnation depth is reported to be lower in mortar samples and mortar joints than in bricks [21,28], and the possibility of cracks after treatment is higher in mortar joints, as well as in the interface between bricks and mortar joints. Moreover, brick absorbs the water repellent agent much faster than mortar [21]. During the application process of the cream products, a percentage of the cream placed in the mortar joints would be absorbed by the brick, leaving less active ingredient for the mortar joints. Furthermore, since the beading effect is reduced due to UV radiation exposure, the water is being absorbed into the first mm of the substrate and during winter this water may freeze, expanding its volume and induce spalling. If this continues to occur and mortar joints start to crumble, cracks may reach untreated areas after years. This could also happen to brick although less possible as the impregnation depth is larger [21]. These observations indicate that mortar joints should be studied further.

The impregnation depth could be increased by applying a higher amount of water repellent agent than recommended and by increasing the concentration of the active ingredient [21]. However, longer curing time and after-treatment water exposure are needed to reveal an improved performance cf. Fig. 4 and [21]. For that reason, the hydrophobic performance of a hydrophobized wall is expected to improve with longer curing time and rain exposure in a period of months after the treatment. Moreover, the water repellency performance should be tested occasionally since re-treatment of substrates is possible [50].

It has been found that the storage properties and the vapor permeability of brick and mortar samples do not significantly change after hydrophobization, although the drying rate of the hydrophobized material is significantly lowered due to the reduced liquid transfer [21,22,56]. The impregnation depth is higher in brick than in mortar and the redistribution of the active ingredient creates a first strong hydrophobic layer and a second area that is partially hydrophobized. The active ingredient continues to spread for many months after treatment increasing the partially hydrophobized area, positively influenced by the after-treatment water exposure [21]. As long as impregnation depth increases, the drying speed of the masonry decreases. For how long the active ingredient could spread inside the material and whether after-treatment water exposure continues to influence the impregnation depth should be addressed in future work.

Material properties are very important in determining the input parameters of hygrothermal simulations, which can be very helpful in the decision-making process to renovate and design a building [57–61]. Hydrophobization is proven to significantly reduce the absorption coefficient of both brick and mortar [21,22,62]. Moreover, hygrothermal simulations using experimental results to imitate the hydrophobic layer illustrate that hydrophobization is the missing element for a moisture-safe energy renovation of internally insulated masonry walls, regardless of the insulation system [10]. But for the hygrothermal simulations to be proven true, the hydrophobic layer should be durable through aging; the absorption coefficient of both brick and mortar should stay at low levels. The fact that absorption coefficient remained at very low levels after artificial aging both in brick and mortar (Fig. 4), in combination with no water-penetration both in the artificially aged samples and the six-year-old hydrophobized mock-up walls (Fig. 5), builds more confidence in the results of the hygrothermal simulations [10]. These results indicate that an internally insulated hydrophobized wall could provide a moisture safe construction. However, high moisture loads from the interior of the building could still be a risk for the wall even when hydrophobization eliminated the wind-driven rain load.

There were two main limitations in this study: firstly, in a wall of a building, there is the interaction between brick and mortar during the contraction/expansion of the materials, or other factors that may induce cracks after treatment, a scenario that is not taken into consideration when performing durability tests on brick and mortar separately. The second limitation is that during the artificial aging the temperature remains constant at 38 °C inside the cabinet and the samples were not exposed to low temperatures in order to investigate the risk of frost damage which may give too optimistic outcome in this study. Moreover, the retrofit of internal insulation increases the frost damage risk [63], thus making the risk of frost damage a very important aspect to be tested.

The current findings have important implications for practitioners and policymakers since the hygrothermal benefits of the combined effect of hydrophobization and internal insulation [10,18,64] can be obtained only if hydrophobization maintains its water repellency performance through aging which needs further studies involving exposure to frost to be fully revealed.

## 5. Conclusions and perspectives

In this paper, the durability of the hydrophobic layer in brick and mortar samples was experimentally studied. The water repellent agents were proven to successfully block capillary effects while avoiding efflorescence at the treated substrate during the process of artificial aging. Karsten tube tests revealed zero water penetration both on hydrophobized samples from artificial aging and on hydrophobized mock-up walls. Moreover, UV radiation was found responsible for the declined beading effect while the after-treatment water exposure seems to influence the water repellency of the treated samples in a positive way since the absorption coefficient is further reduced throughout the procedure of accelerated aging, for all the tested building materials.

Future studies could reveal the frost damage risk in hydrophobized samples compared to untreated. Moreover, future research would benefit from focusing on Karsten tube tests in buildings hydrophobized years ago. Further investigation should include more types of building materials like natural stone and concrete. The results of the current paper and [10] could be used as input in a life cycle cost assessment of hydrophobization in combination with internal insulation which could contribute to a holistic view of hydrophobization.

## Declaration of competing interest

The authors declare that they have no known competing financial interests or personal relationships that could have appeared to influence the work reported in this paper.

## Acknowledgements

The present study is the third journal paper after [10,21] in a series of papers reviewing hydrophobization treatment at BUILD, the Department of the Built Environment, Aalborg University Copenhagen. The study is part of the project 'Moisture safe energy renovation of worth preserving external masonry walls' funded by the Danish foundations: The Landowners' Investment Foundation, The National Building Fund, and Realdania. The authors express sincere thanks to Leif Christiansen (Wewers) for providing the mortars, to Thomas Lenart Svensson (Danish Technological Institute) for cutting the brick samples, to Bravo Miguel (Symtix) for designing and manufacturing with 3D printing the molds for the samples and to Lasse Borgstrøm Eriksen (BUILD) for transporting the samples. We would also like to offer our thanks to Philip Møller (previously Introflex-Remmers), Corne van Hamont (Wacker), and Susanna Stubb-Eliasson (Wacker) for providing water repellent agents.

## References

[1] M. Morelli, M. Harrestrup, S. Svendsen, Method for a component-based economic optimisation in design of whole building renovation versus demolishing and rebuilding, Energy Pol. 65 (2014) 305–314, https://doi.org/10.1016/j.enpol.2013.09.068.
[2] M. Morelli, M.A. Lacasse, A systematic methodology for design of retrofit actions with longevity, J. Build. Phys. 42 (2019) 585–604, https://doi.org/10.1177/1744259118780133.
[3] C.A. Balaras, A.G. Gaglia, E. Georgopoulou, S. Mirasgedis, Y. Sarafidis, D.P. Lalas, European residential buildings and empirical assessment of the Hellenic building stock, energy consumption, emissions and potential energy savings, Build. Environ. 42 (2007) 1298–1314, https://doi.org/10.1016/j.buildenv.2005.11.001.
[4] M. Jerman, I. Palomar, V. Kočí, R. Černý, Thermal and hygric properties of biomaterials suitable for interior thermal insulation systems in historical and traditional buildings, Build. Environ. 154 (2019) 81–88, https://doi.org/10.1016/j.buildenv.2019.03.020.
[5] E. Vereecken, S. Roels, Wooden beam ends in combination with interior insulation: an experimental study on the impact of convective moisture transport, Build, Environ. Times 148 (2019) 524–534, https://doi.org/10.1016/j.buildenv.2018.10.060.
[6] H. Tommerup, S. Svendsen, Energy savings in Danish residential building stock, Energy Build. 38 (2006) 618–626, https://doi.org/10.1016/j.enbuild.2005.08.017.
[7] T. Odgaard, S.P. Bjarløv, C. Rode, Interior insulation – experimental investigation of hygrothermal conditions and damage evaluation of solid masonry façades in a listed building, Build. Environ. 129 (2018) 1–14, https://doi.org/10.1016/j.buildenv.2017.11.015.
[8] M. Morelli, E.B. Møller, Energy savings and risk of mold growth in apartments renovated with internal insulation, Sci. Technol. Built Environ. 25 (2019) 1199–1211, https://doi.org/10.1080/23744731.2019.1629241.
[9] M. Guizzardi, D. Derome, R. Vonbank, J. Carmeliet, Hygrothermal behavior of a massive wall with interior insulation during wetting, Build. Environ. 89 (2015) 59–71, https://doi.org/10.1016/j.buildenv.2015.01.034.
[10] V. Soulios, E.J. de Place Hansen, R. Peuhkuri, Hygrothermal performance of hydrophobized and internally insulated masonry walls - simulating the impact of hydrophobization based on experimental results, Build. Environ. 187 (2021) 107410, https://doi.org/10.1016/j.buildenv.2020.107410.
[11] E. Vereecken, S. Roels, A comparison of the hygric performance of interior insulation systems: a hot box-cold box experiment, Energy Build. 80 (2014) 37–44, https://doi.org/10.1016/j.enbuild.2014.04.033.
[12] E. Vereecken, L. Van Gelder, H. Janssen, S. Roels, Interior insulation for wall retrofitting - a probabilistic analysis of energy savings and hygrothermal risks, Energy Build. 89 (2015) 231–244, https://doi.org/10.1016/j.enbuild.2014.12.031.
[13] X. Zhou, D. Derome, J. Carmeliet, Hygrothermal modeling and evaluation of freeze-thaw damage risk of masonry walls retrofitted with internal insulation, Build. Environ. 125 (2017) 285–298, https://doi.org/10.1016/j.buildenv.2017.08.001.
[14] M. Morelli, S. Svendsen, Investigation of interior post-insulated masonry walls with wooden beam ends, J. Build. Phys. 36 (2013) 265–273, https://doi.org/10.1177/1744259112447928.
[15] H. Janssen, B. Blocken, S. Roels, J. Carmeliet, Wind-driven rain as a boundary condition for HAM simulations: analysis of simplified modelling approaches, Build. Environ. 42 (2007) 1555–1567, https://doi.org/10.1016/j.buildenv.2006.10.001.
[16] A. Nielsen, E.B. Møller, T.V. Rasmussen, E.J. de Place Hansen, Use of sensitivity analysis to evaluate hygrothermal conditions in solid brick walls with interior insulation, in: 5th Int. Build. Phys. Conf., 2012, pp. 377–384. http://vbn.aau.dk/ws/files/72605823/Use_of_sensitivity_analysis_to_evaluate_hygrothermal_conditions_in_solid_brick_walls_with_interior_insulation.pdf.
[17] E. Vereecken, S. Roels, Wooden beam ends in combination with interior insulation: an experimental study on the impact of convective moisture transport, Build, Environ. Times 148 (2019) 524–534, https://doi.org/10.1016/j.buildenv.2018.10.060.
[18] V. Soulios, E.J. de Place Hansen, R. Peuhkuri, Hygrothermal simulation assessment of internal insulation systems for retrofitting a historic Danish building, MATEC Web Conf 282 (2019), 02049, https://doi.org/10.1051/matecconf/201928202049.
[19] V. Metavitsiadis, V. Soulios, H. Janssen, S. Roels, Wall hydrophobization and internal insulation: the impact of impregnation strength and depth on moisture levels and moisture damages, in: Hydrophobe III, 2017, pp. 69–76. http://www.hydrophobe.org/pdf/hongkong/C-1-1.pdf. (Accessed 26 April 2020).
[20] Z. Pavlík, M. Jiřičková, J. Pavlík, R. Černý, Interior thermal insulation system based on hydrophilic mineral wool, J. Therm. Envelope Build. Sci. 29 (2005) 21–35, https://doi.org/10.1177/1744259105051795.
[21] V. Soulios, E.J. de Place Hansen, C. Feng, H. Janssen, Hygric behavior of hydrophobized brick and mortar samples, Build. Environ. 176 (2020) 106843, https://doi.org/10.1016/j.buildenv.2020.106843.
[22] V. Soulios, E.J. de Place Hansen, H. Janssen, Hygric properties of hydrophobized building materials, MATEC Web Conf 282 (2019), 02048, https://doi.org/10.1051/matecconf/201928202048.
[23] J. Engel, P. Heinze, R. Plagge, Adapting hydrophobizing impregnation agents to the object, Hydrophobe VII7th Int. Conf. Water Repel. Treat. Prot. Surf. Technol. Build. Mater. 20 (2014) 141–150, https://doi.org/10.12900/rbm14.20.6-0042.
[24] J. Carmeliet, G. Houvenaghel, J. Van Schijndel, S. Roels, Moisture phenomena in hydrophobic porous building material Part 1: measurements and physical interpretations/Wechselwirkung hydrophobierter poröser Werkstoffe des Bauwesens mit Feuchtigkeit, Teil 1: messungen und physikalische Interpretationen, Restor. Build. Monum. 8 (2002) 165–183, https://doi.org/10.1515/rbm-2002-5660.
[25] E. Vereecken, S. Roels, H. Janssen, Inverse hygric property determination based on dynamic measurements and swarm-intelligence optimisers, Build. Environ. 131 (2018) 184–196, https://doi.org/10.1016/j.buildenv.2017.12.030.
[26] J. Langmans, R. Klein, S. Roels, Hygrothermal risks of using exterior air barrier systems for highly insulated light weight walls: a laboratory investigation, Build. Environ. 56 (2012) 192–202, https://doi.org/10.1016/j.buildenv.2012.03.007.
[27] A.G. Wacker Chemie, Hydrophobic Impregnation with Silres BS, 2014, pp. 1–22.
[28] R.P.J. van Hees, The performance of surface treatments for the conservation of historic brick masonry, Compat. Mater. Prot. Eur. Cult. Herit 2 (1998) 279–287.
[29] E. de Witte, H. De Clercq, R. De Bruyn, A. Pien, Systematic testing of water repellent agents, Restor. Build. Monum. 2 (1996) 133–144, https://doi.org/10.1515/rbm-1996-5093.
[30] H. Brocken, T.G. Nijland, White efflorescence on brick masonry and concrete masonry blocks, with special emphasis on sulfate efflorescence on concrete blocks, Construct. Build. Mater. 18 (2004) 315–323, https://doi.org/10.1016/j.conbuildmat.2004.02.004.
[31] J. Chwast, J. Todorović, H. Janssen, J. Elsen, Gypsum efflorescence on clay brick masonry: field survey and literature study, Construct. Build. Mater. 85 (2015) 57–64, https://doi.org/10.1016/j.conbuildmat.2015.02.094.
[32] B.O. Brandt, T. Van, B. Grelk, K.K. Hansen, S.B. Hansen, Imprægneringsmidlers Indvirkning På Betons Holdbarhed: Del 2: Undersøgelse Af Effekten Af Imprægnering På Kloridindtrængning I Beton Udsat for Varierende Kloridbelastning, 2018.
[33] E.B. Møller, C. Rode, Hygrothermal performance and soiling of exterior building surfaces, Technical University of Denmark, 2004. https://orbit.dtu.dk/files/5285541/byg-r068.pdf.
[34] T.K. Hansen, S.P. Bjarløv, R.H. Peuhkuri, K.K. Hansen, Performance of hydrophobized historic solid masonry – experimental approach, Construct. Build. Mater. 188 (2018) 695–708, https://doi.org/10.1016/j.conbuildmat.2018.08.145.
[35] T. Odgaard, S.P. Bjarløv, C. Rode, Influence of hydrophobation and deliberate thermal bridge on hygrothermal conditions of internally insulated historic solid masonry walls with built-in wood, Energy Build. 173 (2018) 530–546, https://doi.org/10.1016/j.enbuild.2018.05.053.
[36] N.F. Jensen, T.R. Odgaard, S.P. Bjarløv, B. Andersen, C. Rode, E.B. Møller, Hygrothermal assessment of diffusion open insulation systems for interior retrofitting of solid masonry walls, Build. Environ. 182 (2020) 107011, https://doi.org/10.1016/j.buildenv.2020.107011.
[37] N. Feldt Jensen, S.P. Bjarløv, C. Rode, E.B. Møller, Hygrothermal assessment of four insulation systems for interior retrofitting of solid masonry walls through calibrated numerical simulations, Build. Environ. 180 (2020) 107031, https://doi.org/10.1016/j.buildenv.2020.107031.
[38] R. Stenholt-Jacobsen, M.T. Houen, T.L. Christiansen, Air Lime Mortars. Slaking Methods, Workability & Strength Development, Technical University of Denmark, 2019.
[39] Ö. Cizer, K. Van Balen, J. Elsen, D. Van Gemert, Real-time investigation of reaction rate and mineral phase modifications of lime carbonation, Construct. Build. Mater. 35 (2012) 741–751, https://doi.org/10.1016/J.CONBUILDMAT.2012.04.036.
[40] A.G. Remmers, F.C. Funcosil, Technical data sheet, 1–3, https://www.introflex.dk/images/pdf/DK_0711_-_08_13.pdf, 2016.
[41] Wacker Chemie AG, Silres ® bs creme c, Technical data sheet, 4–7, https://www.wacker.com/h/en-us/medias/SILRES-BS-CREME-C-en-2020.07.01.pdf, 2020.

[42] Iso 4892-2:2013, Plastics — Methods of Exposure to Laboratory Light Sources — Part 2: Xenon-Arc Lamps, 2013, p. 13.
[43] Iso 15148 : 2002, Hygrothermal Performance of Building Materials and Products Determination of Water Absorption Coefficient by Partial Immersion, English Version of DIN EN ISO 15148, 2003, pp. 1–14.
[44] C. Feng, H. Janssen, Y. Feng, Q. Meng, Hygric properties of porous building materials: analysis of measurement repeatability and reproducibility, Build, Environ. Times 85 (2015) 160–172, https://doi.org/10.1016/J.BUILDENV.2014.11.036.
[45] C. Feng, H. Janssen, Hygric properties of porous building materials (III): impact factors and data processing methods of the capillary absorption test, Build. Environ. 134 (2018) 21–34, https://doi.org/10.1016/j.buildenv.2018.02.038.
[46] TQC, Karsten tube penetration test ll7500, manual, 1–4, https://mk0tqcsheendm9hfmnd0.kinstacdn.com/wp-content/uploads/2016/05/karsten-tube-penetration-test-li7500-m44.pdf, 2020.
[47] A.F. Stalder, T. Melchior, M. Müller, D. Sage, T. Blu, M. Unser, Low-bond axisymmetric drop shape analysis for surface tension and contact angle measurements of sessile drops, Colloids Surfaces A Physicochem. Eng. Asp. 364 (2010) 72–81, https://doi.org/10.1016/j.colsurfa.2010.04.040.
[48] A.F. Stalder, G. Kulik, D. Sage, L. Barbieri, P. Hoffmann, A snake-based approach to accurate determination of both contact points and contact angles, Colloids Surfaces A Physicochem. Eng. Asp. 286 (2006) 92–103, https://doi.org/10.1016/j.colsurfa.2006.03.008.
[49] M. Rahimi, P. Fojan, L. Gurevich, A. Afshari, Effects of aluminium surface morphology and chemical modification on wettability, Appl. Surf. Sci. 296 (2014) 124–132, https://doi.org/10.1016/j.apsusc.2014.01.059.
[50] L. Courard, V. Lucquiaud, O. Gérard, M. Handy, F. Michel, Evaluation of the durability of hydrophobic treatments on concrete architectural heritage, in: Hydrophobe VII, 2014, pp. 29–38. http://www.hydrophobe.org/pdf/lisboa/VII_03.pdf.
[51] A.E. Charola, Water-repellent treatments for building stones: a practical overview, APT Bull. J. Preserv. Technol. 26 (1995) 10–17, https://doi.org/10.2307/1504480.
[52] R. Asmatulu, G.A. Mahmud, C. Hille, H.E. Misak, Effects of UV degradation on surface hydrophobicity, crack, and thickness of MWCNT-based nanocomposite coatings, Prog. Org. Coating 72 (2011) 553–561, https://doi.org/10.1016/j.porgcoat.2011.06.015.
[53] I.J. De Vries, Hydrophobic treatment, Construct. Build. Mater. 11 (1997) 259–265. https://pdf.sciencedirectassets.com/271475/1-s2.0-S0950061800X00207/1-s2.0-S0950061897000469/main.pdf?X-Amz-Security-Token=IQoJb3JpZ2luX2VjEBQaCXVzLWVhc3QtMSJHMEUCIARwT9fI%2B%2F4uPdwTTbOmg1eV6XRFxUtcnG8%2FzFyEcre0AiEAg7sLvd7Qk7XT7eGJ2ow1dtVV%2B0TguOBEf45L.
[54] P. Freudenberg, Monitoring data basis of European case studies for sound performance evaluation of internal insulation systems under different realistic boundary conditions RIBuild D3.2. https://static1.squarespace.com/static/5e8c2889b5462512e400d1e2/t/5e9db87943530a16d2f414eb/1587394701972/RIBuild_D3.2_v1.0.pdf, 2019.
[55] E.B. Møller, Report on the material properties RIBuild D2.1. https://static1.squarespace.com/static/5e8c2889b5462512e400d1e2/t/5e9db81f43530a16d2f3fecf/1587394609561/RIBuild_D2.1_v1.0.pdf, 2018.
[56] C. Feng, H. Janssen, Impact of water repellent agent concentration on the effect of hydrophobization on building materials, J. Build. Eng. 39 (2021) 102284, https://doi.org/10.1016/j.jobe.2021.102284.
[57] C. Feng, A.S. Guimarães, N. Ramos, L. Sun, D. Gawin, P. Konca, C. Hall, J. Zhao, H. Hirsch, J. Grunewald, M. Fredriksson, K.K. Hansen, Z. Pavlík, A. Hamilton, H. Janssen, Hygric properties of porous building materials (VI): a round robin campaign, Build. Environ. 185 (2020), https://doi.org/10.1016/j.buildenv.2020.107242.
[58] X. Zhou, J. Carmeliet, D. Derome, Influence of envelope properties on interior insulation solutions for masonry walls, Build. Environ. 135 (2018) 246–256, https://doi.org/10.1016/j.buildenv.2018.02.047.
[59] C. Feng, S. Roels, H. Janssen, Towards a more representative assessment of frost damage to porous building materials, Build. Environ. 164 (2019) 106343, https://doi.org/10.1016/j.buildenv.2019.106343.
[60] L. Shi, H. Zhang, Z. Li, X. Man, Y. Wu, C. Zheng, J. Liu, Analysis of moisture buffering effect of straw-based board in civil defence shelters by field measurements and numerical simulations, Build. Environ. 143 (2018) 366–377, https://doi.org/10.1016/j.buildenv.2018.07.018.
[61] L. Havinga, H. Schellen, Applying internal insulation in post-war prefab housing: understanding and mitigating the hygrothermal risks, Build, Environ. Times 144 (2018) 631–647, https://doi.org/10.1016/j.buildenv.2018.08.035.
[62] Y.D. Aktas, H. Zhu, D. D'Ayala, C. Weeks, Impact of surface waterproofing on the performance of brick masonry through the moisture exposure life-cycle, Build. Environ. 197 (2021) 107844, https://doi.org/10.1016/j.buildenv.2021.107844.
[63] P. Johansson, L. Lång, C.-M. Capener, E.B. Møller, E. Quagliarini, M. D'orazio, A. Gianangeli, H. Janssen, C. Feng, J. Langmans, N.F. Jensen, E.J. de Place Hansen, R. Peuhkuri, T.K. Hansen, Threshold values for failure, linked to types of building structures and failure modes RIBuild, AAU, 2019. https://www.ribuild.eu/sites/default/files/media/RIBuild_D2.2_v1.0_1.pdf.
[64] E.J. de Place Hansen, T.K. Hansen, V. Soulios, Deep renovation of an old single-family house including application of an water repellent agent – a case story, in: IOP Conf. Ser. Earth Environ. Sci., 2021, pp. 1–9. https://vbn.aau.dk/files/411162525/427_EJdePlaceHansen_Deep_renovation_of_an_old_single_family_house.pdf.